Ain Shams Engineering Journal (2015) 6, 1093–1104

Ain Shams University

Ain Shams Engineering Journal

www.elsevier.com/locate/asej
www.sciencedirect.com

ENGINEERING PHYSICS AND MATHEMATICS

Unsteady polar fluid model of blood flow through tapered ω-shape stenosed artery: Effects of catheter and velocity slip

D. Srikanth [a,*], J.V. Ramana Reddy [a], Shubha Jain [a], Anup Kale [b]

[a] *Department of Applied Mathematics, Defence Institute of Advanced Technology (DU), Pune 411025, India*
[b] *Department of Bio-science Engineering, Defence Institute of Advanced Technology (DU), Pune 411025, India*

Received 10 August 2014; revised 11 December 2014; accepted 7 January 2015
Available online 24 March 2015

KEYWORDS

Couple stress fluid;
Blood flow;
Tapered artery;
Catheter;
Slip velocity

Abstract In this paper, we considered the pulsatile flow of blood through catheterized tapered artery in the presence of an ω-shaped stenosis. Blood flow is modelled as homogeneous incompressible couple stress fluid. Further the effects of velocity slip at the arterial wall are also examined. The analysis is carried out analytically and closed form solutions are obtained with the assumption of mild stenosis. In the present study, we analyze the effects of various fluid and geometric parameters on the physiological parameters such as resistance to flow and shear stress at the wall. The variation in the resistance to the flow and wall shear stress with respect to stenosis size (ϵ, ψ), radius of the catheter (R_c), couple stress fluid parameters (β, ω), Reynolds number (Re) and pulsatile parameter (σ) has been studied. In particular shear stress at the wall is reckoned at both the locations corresponding to the maximum height of the stenosis. It has been observed that this physiological parameter is independent of the location of the maximum height in case of nontapered artery while these locations significantly impact the shear stress at the wall in case of tapered artery. The locations of the critical and maximum heights with corresponding annular radii are summarized in the form of Table 1. We also focussed our attention on the analysis of the wall shear stress over the entire stenosis region for various values of the geometric and fluid parameters. It is observed that the impedance and wall shear stress are increasing with increase in the radius of catheter and stenosis size while they are decreasing as the tapered parameter and the couple stress fluid parameters are increasing. It is observed that slip velocity and diverging tapered artery facilitate the fluid flow.

* Corresponding author. Tel.: +91 7798229930.
E-mail address: sri_dasari1977@yahoo.co.in (D. Srikanth).
Peer review under responsibility of Ain Shams University.

Production and hosting by Elsevier

1. Introduction

Cardiovascular diseases (CVDs) are the group of disorders of heart and blood vessels. CVDs include coronary heart disease, cerebrovascular disease, peripheral arterial disease, rheumatic heart disease, congenital heart disease and deep vein

http://dx.doi.org/10.1016/j.asej.2015.01.003
2090-4479

thrombosis and pulmonary embolism. Over the period of past few decades it has been the leading cause of death worldwide [1]. Lot of research efforts are going on to prevent, control and cure these disorders. Most of the deaths occur because of heart attacks and strokes apart from conditions of ischaemia, atherosclerosis and thrombosis. Heart attacks and strokes are usually acute events mainly caused by blockage/s that prevent the flowing of blood to the heart or brain. The build-up of fatty deposits on the inner walls of the blood vessels, that supply blood to the heart or brain is one of the most-common causes. Strokes can be caused by bleeding from a blood vessel in the brain or from blood clots. The abnormal narrowing of blood vessels in various locations of cardiovascular system due to the deposition of the cholesterol and other fatty substances leads to a medical condition called as stenosis [2]. Stenoses lead to circulatory disorders such as atherosclerosis. The ethological studies on stenosis suggest that deposition of calcium, fatty components and cholesterol on the inner walls of the artery prevent the flowing of blood leading to rupture of the artery and thrombosis. Thrombus can form emboli which occlude the smaller vessels.

The dynamics of the blood flow is drastically affected in all these conditions and has adverse effects on the blood circulation and its control by cardiovascular system. Stenosis increases the resistance to the flow of blood in arteries resulting in increased blood pressure. It is now a well established fact that stenosis induces substantial changes in blood flow velocity, pressure distribution, wall shear stress and impedance. Currently most of these conditions cannot be detected in routine check-ups and CT scan remains a major technique to diagnose stenosis conditions. It is imperative to understand the behaviour of blood flow in a stenosed artery which is quite different in comparison to the normal ones. Information about the flow parameters such as velocity, flow rate, pressure drop in diseased vessel can be crucial and can help to save the further fatality and prevent the occurrence of the disease. It can help patients to get right treatment at right time. The mathematical modelling and numerical simulation studies have the huge potential and can very well interpret existing in vivo data and eventually help in the improved diagnosis. The assumptions of blood flow parameters made from mathematical modelling can be crucial and life saving. In this paper we try to model the blood flow in stenosed artery to understand the behaviour of blood and connect it to the possible leading medical condition.

Initial understanding of blood flow dynamics was done by considering blood as a Newtonian fluid [3–5]. But theoretical and experimental investigations indicated that blood cannot be treated as a single phase homogeneous viscous fluid while flowing through small arteries [6,7]. It is now well established that blood is a suspension of corpuscles (cellular particles) in an aqueous saline solution of plasma which indicates that blood is having a non-Newtonian structure. Siddiqui et al. [8] have investigated the pulsatile nature of blood by modelling blood as a Casson fluid. They observed that the yield stress increases with a decrease in the mean and steady flow rates. Sankar et al. [9] observed the effects of non-symmetric stenosis on the physiological properties of the flow by treating blood as Herschel Bulkley fluid. Varshney et al. [10] noticed the effect of time-dependent radius of the artery on flow rate, wall shear stress, etc., by considering the blood as power-law fluid. The influence of heat and mass transfer on blood flow through asymmetric stenosis was discussed by Akbar et al. [11,12], where in blood is modelled as Jefferey fluid and Sisko fluid respectively. A perturbation method was used to examine biomechanical analysis of Prandtl fluid flow through stenosed tapered artery by Akbar et al. [13].

Chakravarty et al. [14] have studied about the two dimensional blood flow through tapered arteries under stenotic condition. They mentioned that in most of the earlier studies, flow in the arteries has been considered in cylindrical tubes with uniform cross section. But in reality bifurcation of blood vessels at frequent intervals and variation in the vessel diameter with distance is well known and the most of the vessels could be considered as long, narrow and slowly tapering cones. Noreen et al. [15] have analysed the effects of vessel tapering together with the asymmetric stenosed tapered artery on the flow characteristics by considering blood as a Nano fluid. Here authors concluded that velocity profile is rising with the increase in slip velocity. Peristaltic Newtonian fluid of chyme flow through small intestine was modelled by Akbar et al. [16].

There are many treatments available for diagnosing and treating constricted vessels. Catheterization (thin, flexible tube) is one of them, in which balloon angioplasty is a specialized form of catheterization. These procedures are widely used in the medical field for treating the atherosclerosis. Insertion of the catheter in a tube creates an annular region between inner wall of the artery and outer wall of the catheter which influences the flow field such as pressure distribution, shear stress at the wall, resistance to flow (impedance). In view of its immense importance, the effect of the catheter on physiological parameters was discussed by the researchers [17,18]. In particular they considered pulsatile nature of blood flow when blood is modelled as non-Newtonian fluid.

The shapes of the stenosis in the above aforesaid studies have been considered to be radially symmetric or asymmetric. But while stenosis is maturing it may grow up in series manner, overlap with each other and it would be appear like ω-shape. Daniel et al. [19] observed the pressure gradient force, flow velocity, impedance and wall shear stress in the overlapping stenotic zone at the critical height and at the throats of such stenosis. Here they considered steady nature of flow. Srivastava et al. [20] explored the arterial blood flow through an overlapping stenosis by treating the blood as a Casson fluid. They figured impedance and shear stress for different stenosis heights. Chakravarty et al. [21] discussed the effects of the overlapping stenosis under low shear rate flow.

The presence of red cell slip at the vessel wall was recommended theoretically by Vand [22], experimentally by Bunnett [23] and Nubar [24], Chaturani et al. [25], etc. They used slip velocity at the wall in their analysis. Lately, Ponalagusamy [26], Biswas et al. [27] and Ponalagusamy [28] have developed mathematical models for blood flow through stenosed arterial segment, by taking a velocity slip condition at the constricted wall. The extensive discussion on symmetric and asymmetric slip velocity at the wall was done by Ghosh et al. [29]. Thus, it is very appropriate to consider velocity slip at the wall of the stenosed artery in blood flow modeling.

In the stenosed condition, substantial reduction in the lumen of an artery results in size effects (ratio of haematocrit to vessel diameter), which influences flow characteristics significantly. To study the size effect in the fluid flow, Stokes [30], Eringen [31] and Cowin [32] have proposed continuum

model. Micro-continuum structure of the fluid is also referred as couple stress fluid which is proposed by Stokes. The foreground of couple stress fluid is to introduce size dependent effects as mentioned above that is not present in other classical viscous fluids. Because of its mathematical simplicity it has been widely used by number of researchers [33–36].

With the above motivation, an attempt has been made to study the effects of ω-shaped stenosis on the physiological parameters of the blood flow that is modelled as couple stress fluid through a catheterized tapered artery. Velocity slip at the wall is additionally thought of. The analysis is done analytically and the results are shown diagrammatically. This configuration with the related results could be very useful in the development of various related technologies, Biomedical equipments and also to those who are engaged in the design and development of artificial organs.

2. Formulation of the problem

Mathematical model of blood flow through an ω-shaped stenosed arterial segment through a tapered artery in the presence of catheter is to be built to study the impact of various geometric and fluid parameters on physiological parameters. In particular modelling is to be done by considering incompressible homogeneous couple stress fluid to represent blood. The geometry of the ω-shaped stenosis is shown in Fig. 1 and is expressed mathematically with inputs from [19–21] as

$$h(z)=\begin{cases}(R_0+\zeta z)-\frac{3}{2}\frac{\epsilon}{R_0L_1^4}\Big[11(z-L_0)L_1^3-47(z-L_0)^2L_1^2\\ +72(z-L_0)^3L_1-36(z-L_0)^4\Big], L_0\leqslant z\leqslant L_0+L_1\\ (R_0+\zeta z), \qquad\qquad \text{otherwise}\end{cases}$$

where R_0 is the radius of the annular region in case of nontapered artery in the nonconstricted domain, R_c is the radius of the catheter, L_1 is the stenosis length, L_0 indicates the location of stenosis, ϵ is the maximum height of the stenosis into the lumen, $\zeta(=\tan\theta)$ is the tapering parameter which represents the slope of the tapered vessel with θ being the tapering angle. $\phi<0$, $\phi>0$ and $\phi=0$ are for converging taper, diverging taper and no-taper respectively. z_1 and z_3 are the left and right locations on the axial line where the maximum height of the stenosis is occurring and z_2 represents the location on z axis corresponding to the critical height of the ω-shaped stenosis.

The governing equations which describes the couple stress fluid:

$$\frac{D\rho}{Dt}+\rho(\nabla\cdot\overline{V})=0 \tag{1}$$

$$\rho\frac{D\overline{V}}{Dt}=-\nabla P+(\lambda+\mu)\nabla\nabla\cdot\overline{V}+\eta\nabla^2\nabla\nabla\cdot\overline{V}-\eta\nabla^4\overline{V}+\mu\nabla^2\overline{V}+\rho\bar{f}+\frac{1}{2}\nabla\times(\rho\bar{l}) \tag{2}$$

For couple stress fluid shear stress tensor is not symmetric. The force stress tensor (τ) and the couple stress tensor (M) that arises in the theory of couple stress fluids are given by

$$\tau=(-P+\lambda\nabla\overline{V})\,I+\mu\Big[\nabla\overline{V}+(\nabla\overline{V})^T\Big]+\frac{1}{2}I\times[\nabla M+\rho C] \tag{3}$$

and

$$M=m\,I+2\eta\,(\nabla(\nabla\times\overline{V}))\;+\;2\eta'(\nabla(\nabla\times\overline{V}))^T \tag{4}$$

where ρ is the density, $\overline{V}$ is velocity vector, P is the pressure, λ and μ are the viscosity coefficients, η and η' are couple stress coefficients. f is a body force and l is a body couple moment. Further the materials constants μ,λ,η and η' satisfy the inequalities

$$\mu\geqslant 0,\quad 3\lambda+2\mu\geqslant 0,\quad \eta\geqslant 0,\quad \eta\geqslant\eta'$$

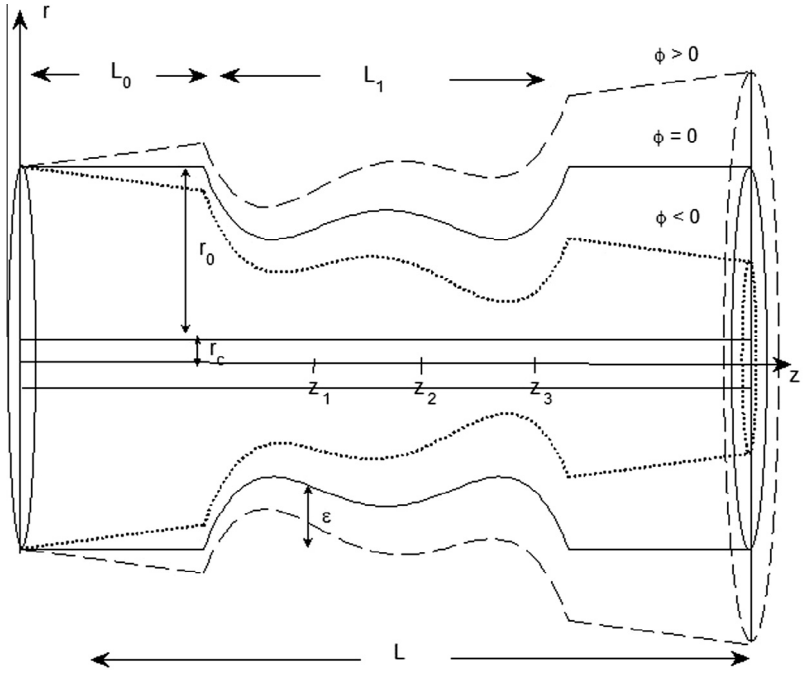

Figure 1 Schematic representation of the geometry.

The flow of homogeneous incompressible couple stress fluid, in the absence of body force and body couple moment the above field Eqs. (1) and (2) reduce to

$$\nabla \cdot \overline{V} = 0 \tag{5}$$

$$\rho\left[\frac{\partial \overline{V}}{\partial t} + (\overline{V}\cdot\nabla)\overline{V}\right] = -\nabla P - \eta\nabla^4\overline{V} + \mu\nabla^2\overline{V} \tag{6}$$

The problem has been studied in cylindrical polar coordinate system (r, θ, z). Since the flow is assumed axisymmetric, all the variables are independent of θ. The velocity vector $\overline{V} = (u, 0, w)$, where u and w are functions of r, z and t. After the coordinate transformation, the Eqs. (5) and (6) get transformed into,

$$\frac{\partial u}{\partial r} + \frac{u}{r} + \frac{\partial w}{\partial z} = 0 \tag{7}$$

$\overline{r}$ component

$$\begin{aligned}\rho\left(\frac{\partial u}{\partial t} + u\frac{\partial u}{\partial r} + w\frac{\partial u}{\partial z}\right) &= -\frac{\partial P}{\partial r} + \mu\left(\frac{\partial^2 u}{\partial r^2} + \frac{1}{r}\frac{\partial u}{\partial r} - \frac{u}{r^2} + \frac{\partial^2 u}{\partial z^2}\right)\\ &\quad - \eta\left(\frac{\partial^4 u}{\partial r^4} + 2\frac{\partial^4 u}{\partial r^2\partial z^2} + \frac{\partial^4 u}{\partial z^4} + \frac{2}{r}\frac{\partial^3 u}{\partial r^3}\right.\\ &\quad + \frac{2}{r}\frac{\partial^3 u}{\partial r\partial z^2} - \frac{3}{r^2}\frac{\partial^2 u}{\partial r^2} - \frac{2}{r^2}\frac{\partial^2 u}{\partial z^2}\\ &\quad \left. + \frac{3}{r^3}\frac{\partial u}{\partial r} - \frac{3}{r^4}u\right)\end{aligned} \tag{8}$$

$\overline{z}$ component

$$\begin{aligned}\rho\left(\frac{\partial w}{\partial t} + u\frac{\partial w}{\partial r} + w\frac{\partial w}{\partial z}\right) &= -\frac{\partial P}{\partial z} + \mu\left(\frac{\partial^2 w}{\partial r^2} + \frac{1}{r}\frac{\partial w}{\partial r} + \frac{\partial^2 w}{\partial z^2}\right)\\ &\quad - \eta\left(\frac{\partial^4 w}{\partial r^4} + 2\frac{\partial^4 w}{\partial r^2\partial z^2} + \frac{\partial^4 w}{\partial z^4} + \frac{2}{r}\frac{\partial^3 w}{\partial r^3}\right.\\ &\quad \left. + \frac{2}{r}\frac{\partial^3 w}{\partial z^2\partial r} - \frac{1}{r^2}\frac{\partial^2 w}{\partial r^2} + \frac{1}{r^3}\frac{\partial w}{\partial r}\right)\end{aligned} \tag{9}$$

The above Eqs. (8) and (9) are the r and z component of the Eq. (6) respectively.

The non-dimensional parameters are obtained as follows:

$$r' = \frac{r}{R_0}, \quad w' = \frac{w}{u_0}, \quad z' = \frac{z}{L_1}, \quad u' = \frac{L_1 u}{u_0\epsilon},$$
$$\epsilon' = \frac{\epsilon}{R_0}, \quad t' = \Omega t, \quad h' = \frac{h}{R_0}, \quad \lambda' = \frac{\lambda}{L},$$
$$\zeta' = \frac{\zeta L_1}{R_0}, \quad h' = \frac{h}{R_0}, \quad P' = \frac{R_0^2 P}{u_0 L_1 \mu}, \quad \tau' = \tau\frac{R_0}{\mu u_0}$$

The non-dimensional form of the geometry of stenosis, after dropping the dashes is

$$h(z) = \begin{cases} (1+\zeta z) - \frac{3\epsilon}{2}[11(z-\alpha) - 47(z-\alpha)^2 \\ \quad +72(z-\alpha)^3 - 36(z-\alpha)^4], & \alpha \leqslant z \leqslant \alpha+1 \\ (1+\zeta z), & \text{otherwise} \end{cases} \tag{10}$$

where $\alpha = \frac{L_0}{L_1}, u_0$ is typical axial velocity, Ω is the circular frequency.

In Table 1, the location of the extremum heights of the stenosis (z_1, z_2, z_3) and the corresponding radius of the annular region for various values of the tapered parameter ζ are numerically calculated with fixed values of $L = 2, R_0 = 1$, $L_1 = L/2$, $L_0 = (L - L_1)/2$ summarized.

Using non-dimensional parameters in the Eqs. (7)–(9) we get,

$$\gamma\left(\frac{\partial u}{\partial r} + \frac{u}{r}\right) + \frac{\partial w}{\partial z} = 0 \tag{11}$$

$$\begin{aligned} &Re\sigma\gamma^2\delta^2\frac{\partial u}{\partial t} + Re\,\gamma\delta^3\left(\gamma u\frac{\partial u}{\partial r} + w\frac{\partial u}{\partial z}\right)\\ &= -\frac{\partial P}{\partial r} + \gamma\delta^2\left(\frac{\partial^2 u}{\partial r^2} - \frac{u}{r^2} + \frac{1}{r}\frac{\partial u}{\partial r} + \delta^2\frac{\partial^2 u}{\partial z^2}\right)\\ &\quad - \frac{\gamma\delta^2}{\beta^2}\left[\frac{\partial^4 u}{\partial r^4} + \frac{2}{r}\frac{\partial^3 u}{\partial r^3} - \frac{3}{r^2}\frac{\partial^2 u}{\partial r^2} + \frac{3}{r^3}\frac{\partial u}{\partial r} - \frac{3}{r^4}u\right.\\ &\quad \left. + \delta^2\left(2\frac{\partial^4 u}{\partial r^2\partial z^2} + \delta^2\frac{\partial^4 u}{\partial z^4} + \frac{2}{r}\frac{\partial^3 u}{\partial r\partial z^2} - \frac{2}{r^2}\frac{\partial^2 u}{\partial z^2}\right)\right]\end{aligned} \tag{12}$$

$$\begin{aligned} &Re\,\sigma\frac{\partial w}{\partial t} + Re\,\delta\left(\gamma u\frac{\partial w}{\partial r} + w\frac{\partial w}{\partial z}\right)\\ &= -\frac{\partial P}{\partial z} + \left(\frac{\partial^2 w}{\partial r^2} + \frac{1}{r}\frac{\partial w}{\partial r} + \delta^2\frac{\partial^2 w}{\partial z^2}\right)\\ &\quad - \frac{1}{\beta^2}\left[\frac{\partial^4 w}{\partial r^4} + \frac{2}{r}\frac{\partial^3 v_z}{\partial r^3} - \frac{1}{r^2}\frac{\partial^2 w}{\partial r^2} + \frac{1}{r^3}\frac{\partial w}{\partial r} + \delta^4\frac{\partial^4 w}{\partial z^4}\right.\\ &\quad \left. + 2\delta^2\left(\frac{\partial^4 w}{\partial r^2\partial z^2} + \frac{1}{r}\frac{\partial^3 w}{\partial z^2\partial r}\right)\right]\end{aligned} \tag{13}$$

where $\gamma = \epsilon/R_0$, $\delta = R_0/L_1$, $Re = \rho u_0 R_0/\mu$ is the Reynolds number, $\beta = R_0\sqrt{\mu/\eta}$ is the couple stress fluid parameter and the pulsatile parameter is $\sigma = R_0\Omega/u_0$.

Under the assumption of mild stenosis i.e., $\gamma(= \epsilon/R_0) \ll 1$ and further assuming that $\delta(= R_0/L_1) \approx O(1)$, Eqs. (12) and (13) get transformed into

$$\frac{\partial P}{\partial r} = 0 \tag{14}$$

$$\begin{aligned} Re\,\sigma\frac{\partial w}{\partial t} &= -\frac{\partial P}{\partial z} + \left(\frac{\partial^2 w}{\partial r^2} + \frac{1}{r}\frac{\partial w}{\partial r}\right)\\ &\quad - \frac{1}{\beta^2}\left[\frac{\partial^4 w}{\partial r^4} + \frac{2}{r}\frac{\partial^3 w}{\partial r^3} - \frac{1}{r^2}\frac{\partial^2 w}{\partial r^2} + \frac{1}{r^3}\frac{\partial w}{\partial r}\right]\end{aligned} \tag{15}$$

Let $D^2 = \frac{\partial^2}{\partial r^2} + \frac{1}{r}\frac{\partial}{\partial r}$, then the Eq. (15) can be written as

$$Re\,\sigma\frac{\partial w}{\partial t} = -\frac{\partial P}{\partial z} + D^2 w - \frac{1}{\beta^2}D^4 w \tag{16}$$

The corresponding non-dimensional boundary conditions are as shown below

$$\begin{aligned} &w = v \quad \text{at} \quad r = h(z)\\ &w = 0 \quad \text{at} \quad r = R_c\\ &\frac{\partial^2 w}{\partial r^2} - \frac{\omega}{r}\frac{\partial w}{\partial r} = 0 \quad \text{at} \quad r = h(z)\ \&\ r = R_c \end{aligned} \tag{17}$$

Here v is the slip velocity at the wall of the artery and no slip at the catheter wall is considered. $\omega = \eta'/\eta$ is the couple stress fluid parameter. ω is the parameter which accounts for the effect of local viscosity due to particles in addition to bulk viscosity of the fluid (μ). The effects of couple stresses will be absent in a material for which $\eta = \eta'$. This is equivalent to requiring that the couple stress tensor be symmetric. If couple stress tensor is symmetric, then the Eq. (17) shows that, the couple stresses are vanishing at the wall of the artery and the

Table 1 Locations of the extremum height of the stenosis.

ζ	Location of z	$h(z)$ for fixed value of $\epsilon = 0.1$
0.005	$z_1 = 0.6876$	0.8774
	$z_2 = 1.0012$	0.9300
	$z_3 = 1.3112$	0.8805
0	$z_1 = 0.6882$	0.8740
	$z_2 = 1.0000$	0.9250
	$z_3 = 1.3118$	0.8740
−0.005	$z_1 = 0.6888$	0.8705
	$z_2 = 0.9988$	0.9200
	$z_3 = 1.3124$	0.8674

catheter, as the mechanical interactions at the wall are equipollent to a force distribution only.

3. Solution of the problem

As the flow considered is pulsatile in nature and using the fact that the Eqs. (14) and (16) are linear, it is appropriate to consider the solution as [18]

$$w(r,z,t) = \mathrm{Re}(w^*(r,z)\,e^{it}), \quad P(r,z,t) = \mathrm{Re}(P^*(r,z)\,e^{it}) \tag{18}$$

By using Eq. (18), the Eqs. (14) and (16) become,

$$\frac{\partial P^*}{\partial r} = 0 \tag{19}$$

$$D^4 w^* - \beta^2 D^2 w^* + iRe\sigma\beta^2 w^* = -\beta^2 \frac{\partial P^*}{\partial z} \tag{20}$$

Let, $n_1^2 + n_2^2 = \beta^2$ and $n_1^2 * n_2^2 = iRe\,\sigma\beta^2$ then Eq. (20) is simplified to the form,

$$(D^2 - n_1^2)(D^2 - n_2^2)w^* = -\beta^2 \frac{\partial P^*}{\partial z} \tag{21}$$

The solution of above equation is

$$w^* = c_1(z)I_0(n_1 r) + c_2(z)K_0(n_1 r) + c_3(z)I_0(n_2 r) + c_4(z)K_0(n_2 r) - \frac{1}{iRe\sigma}\frac{\partial P^*}{\partial z} \tag{22}$$

where $I_0(n_i r)$ and $K_0(n_i r)$ are modified Bessel function of order zero of first and second kind respectively (for $i = 1, 2$). c_i for $i = 1, 2, 3, 4$ are calculated by using boundary conditions.

Therefore, the non-dimensional volumetric flow rate (Q) across the radial distance is expressed as,

$$Q = \int_{R_c}^{h(z)} 2\,r\,w^*\,dr \tag{23}$$

is obtained in the form $Q = 2\,\frac{\partial P^*}{\partial z}\,F[h(z), R_c]$, where

$$F[h(z),R_c] = \frac{d_1}{n_1}(hI_1[n_1 h] - R_c I_1[n_1 R_c]) + \frac{d_2}{n_1}(R_c K_1[n_1 R_c] - hK_1[n_1 h]) + \frac{d_3}{n_2}(hI_1[n_2 h] - R_c I_1[n_2 R_c]) + \frac{d_4}{n_2}(R_c K_1[n_2 R_c] - hK_1[n_2 h]) - \frac{h^2 - R_c^2}{2iRe\sigma} \tag{24}$$

where $\frac{\partial P^*}{\partial z} d_i = c_i$, for $i = 1, 2, 3, 4$. The pressure drop ΔP across the stenosis between the sections $z = 0$ and $z = L$ is obtained by $\Delta P = \frac{Q}{2}\int_0^L \frac{1}{F[h(z),R_c]}dz$.

3.1. Resistance to flow (Impedance)

The impedance depends on flow rate of the fluid and variation in pressure drop. Hence it is very important to analyse the resistance to the flow, influenced by different fluid and geometry parameters. The resistance to the flow is calculated as $\lambda = \frac{\Delta P}{Q}$

$$\lambda = \frac{1}{2}\int_0^L \frac{1}{F[h(z),R_c]}dz$$

$$\lambda = \frac{1}{2}\left[\int_0^{L_0} \frac{1}{F[h(z),R_c]}dz + \int_{L_0}^{L_0+L_1} \frac{1}{F[h(z),R_c]}dz + \int_{L_0+L_1}^{L} \frac{1}{F[h(z),R_c]}dz\right] \tag{25}$$

The non-dimensional form of resistance to flow is given by

$$\lambda = \frac{\psi}{2}\left[\int_0^{\alpha} \frac{1}{F[h,R_c]}dz + \int_{\alpha}^{\alpha+1} \frac{1}{F[h,R_c]}dz + \int_{\alpha+1}^{\frac{1}{\psi}} \frac{1}{F[h,R_c]}dz\right] \tag{26}$$

where $\psi = \frac{L_1}{L}$, $\alpha = \frac{L_0}{L_1}$

3.2. Wall shear stress

Since shear stress at the wall significantly influences the flow characteristics and rate of mass transport across the artery wall, our prime objective of the problem is to evaluate wall shear stress in the constricted artery.

The shear stress (τ_{rz}) is the sum of symmetric and antisymmetric parts and is calculated at the wall of the stenosed artery using the follow expression

$$\tau_{rz} = \tau_{rz}^S + \tau_{rz}^A \tag{27}$$

where the symmetric part (τ_{rz}^S) and antisymmetric part (τ_{rz}^A) of the stresses are given as

$$\tau_{rz}^S = \mu\frac{\partial w}{\partial r}$$

and

$$\tau_{rz}^A = \frac{1}{2}\left(\frac{\partial m_{r\theta}}{\partial r} + \frac{m_{r\theta} + m_{\theta r}}{r}\right)$$

where the couple stress components $m_{r\theta}$ and $m_{\theta r}$ are expressed as

$$m_{r\theta} = \frac{1}{2}\left(-\eta\frac{\partial^2 w}{\partial r^2} + \frac{\eta'}{r}\frac{\partial w}{\partial r}\right) \quad \text{and} \quad m_{\theta r} = \frac{1}{2}\left(-\eta'\frac{\partial^2 w}{\partial r^2} + \frac{\eta}{r}\frac{\partial w}{\partial r}\right)$$

Substituting these expressions and using the Eq. (3), the non-dimensional total shear stress at the wall is given by

$$\tau_w = n_1(c_1 I_1(n_1 r) - c_2 K_1(n_1 r))\left(1 - \frac{n_1^2}{4(n_1^2 + n_2^2)}\right) + n_2(c_3 I_1(n_2 r) - c_4 K_1(n_2 r))\left(1 - \frac{n_2^2}{4(n_1^2 + n_2^2)}\right) \tag{28}$$

Wall shear stress is calculated in the stenosis region and at the extreme heights of the stenosis, the locations of which can be obtained from Eq. (10) by using simple calculus.

4. Results and discussion

During the formulation and solution, the locations on the axial axis corresponding to the maximum height of the stenosis which are dependent on the tapered parameter are computed and summarized in Table 1. Further resistance to the flow and wall shear stress at the extreme heights of the stenosis and across the entire length of the stenosis are computed. In this section we discuss our results corresponding to various fluid and geometry parameters such as the tapered parameter (ζ), radius of the catheter (R_c), height of the stenosis (ϵ), the couple stress fluid parameters (β, ω), Reynolds number (Re), Strouhal number (σ) and slip velocity (v) on physiological parameters impedance and shear stress at the wall. It is reported [37] that fluid near the wall is moving slowly or can be stopped which creates reverse flow against the main stream flow and separate the main stream from the wall i.e., separation of flow. In the present analysis, it has been observed that the impedance and wall shear stress are decreasing and are negative for a short period of time before again becoming positive. The brief period for which the physiological parameter is negative before becoming positive is corresponding to separation of flow [2]. As a matter of fact the major separation is settled near the maximum height of stenosis when the stenosis is moderate, very severe or of slowly growing type [38]. It is clear that the flow rate will be smaller for higher impedance. Also the volume of fluid flow in the artery is determined by the resistance to the flow. Fig. 2 represents the variation of impedance with respect to time in case of tapered parameter (ζ). It is observed that in case of converging artery impedance is highest and it keeps on decreasing as the artery diverges. Accordingly it can be concluded that impedance increases as the artery is converging. All the future results are obtained in case of converging tapered artery.

Effect of radius of catheter (R_c) on the impedance is figured out with the fixed value of other parameters and is presented in Fig. 3. It is observed that the annular region of artery gets reduced with the increment in the radius of catheter, that results in higher pressure distribution which further results in increase in the resistance to the flow. Hence, catheter has immense effect on the flow characteristics. In Fig. 4, effect of height of stenosis (ϵ) on impedance is analysed. Here impedance increases as the height of the constriction grows in the artery. Further the effect of length of the stenosis (ψ) is

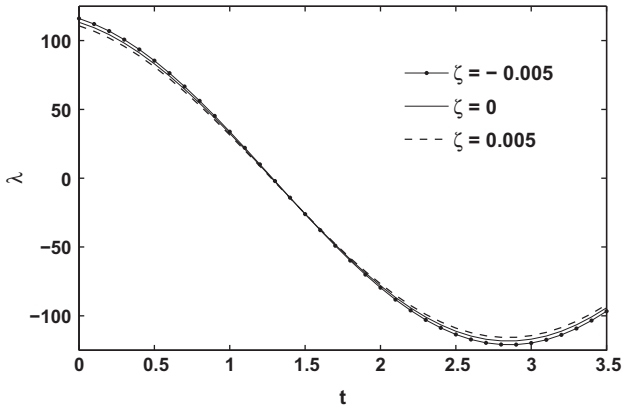

Figure 2 The variation in the resistance to the flow with respect to ζ with $\beta = 1.5, \sigma = 3, Re = 10, \epsilon = 0.1, \omega = 0.2, \gamma = 0.5, v = 0.0001, R_c = 0.1$.

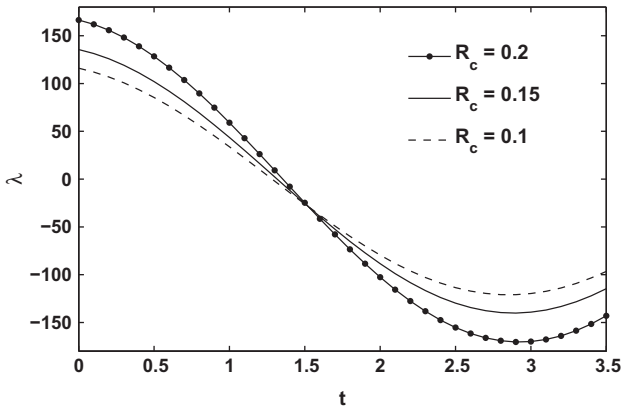

Figure 3 The variation in the resistance to the flow with respect to R_c with $\beta = 1.5, \sigma = 3, Re = 10, \epsilon = 0.1, \omega = 0.2, \psi = 0.5, v = 0.0001, \zeta = -0.005$.

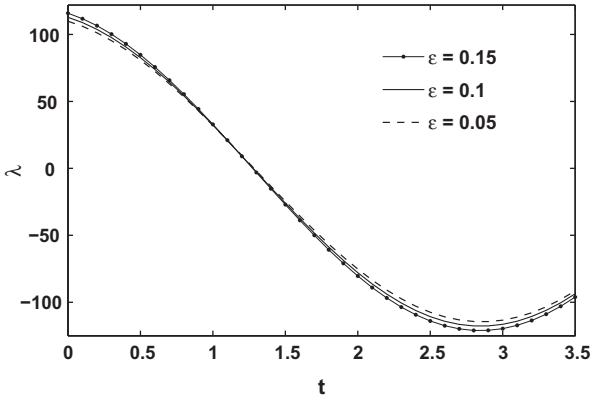

Figure 4 The variation in the resistance to the flow with respect to ϵ with $\zeta = -0.005, \psi = 0.5, \beta = 1.5, \sigma = 3, Re = 10, \omega = 0.2, v = 0.0001, R_c = 0.1$.

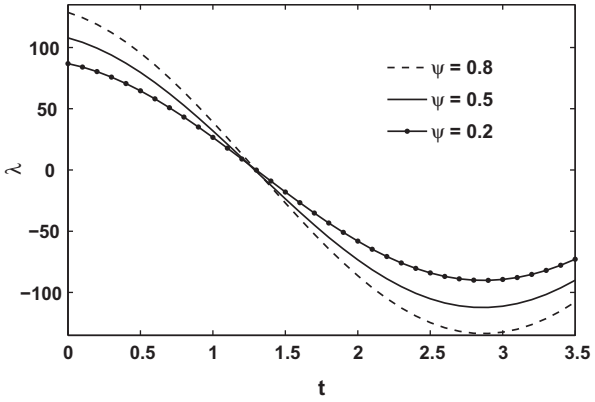

Figure 5 The variation in the resistance to the flow with respect to ψ with $\beta = 1.5, \sigma = 3, Re = 10, \epsilon = 0.1, \omega = 0.2, \zeta = -0.005, v = 0.0001, R_c = 0.1$.

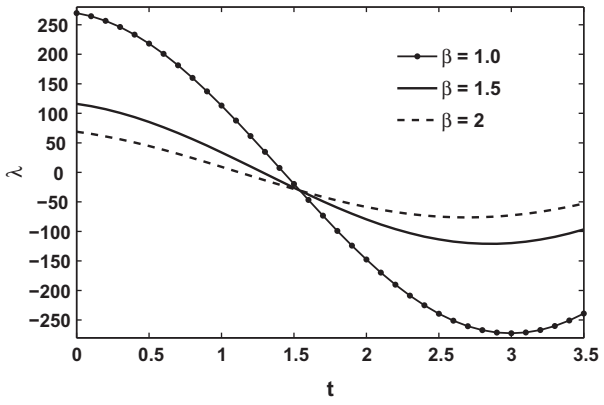

Figure 6 The variation in the resistance to the flow with respect to β with $\psi = 0.5, \sigma = 3, Re = 10, \epsilon = 0.1, \omega = 0.2, \zeta = -0.005, \nu = 0.0001, R_c = 0.1$.

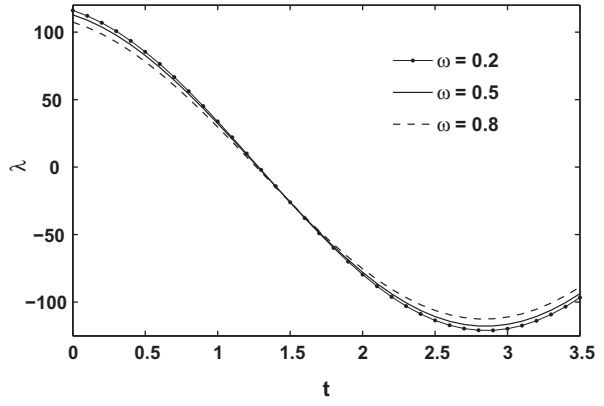

Figure 7 The variation in the resistance to the flow with respect to ω with $\psi = 0.5, \beta = 1.5, \sigma = 3, Re = 10, \epsilon = 0.1, \zeta = -0.005, \nu = 0.0001, R_c = 0.1$.

observed in Fig. 5. Due to the constriction proliferation in the intima, there is an increase in the resistance to the flow as a result of large fluctuations in the pressure difference.

The couple stress fluid parameter (β) gives the size dependent effect on the impedance. Non-polar theory does not predict size dependent effects. Hence modelling blood by a polar fluid like couple stress fluid is very appropriate. As shown in Fig. 6, impedance increases as the couple stress fluid parameter (β) decreases. It is to be noted as $\beta \to \infty$, properties of couple stresses in the fluid vanish and hence behaves like a Newtonian fluid. Hence it is understood that impedance is more in couple stress fluid when compared to that of Newtonian fluid. The effect of another parameter (ω) arising out of the fluid considered is shown in Fig. 7, from which it is observed that impedance and ω are inversely related. This is true because, the couple stress tensor effects will be absent when $\omega \to 1$. The couple stress components become equal as $\omega \to 1$ (i.e., $\eta = \eta'$) and further because of the boundary condition (17) it becomes zero. Hence shear stress becomes symmetric as skew-symmetric part of shear stress becomes zero. Hence it is justified that the presence of couple stresses increases the impedance.

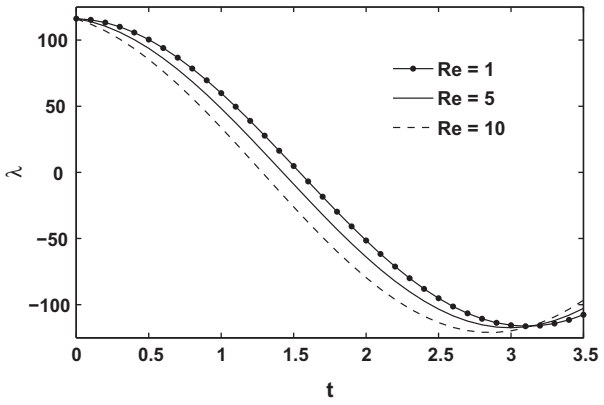

Figure 8 The variation in the resistance to the flow with respect to Re with $\psi = 0.5, \beta = 1.5, \sigma = 3, \epsilon = 0.1, \omega = 0.2, \zeta = -0.005, \nu = 0.0001, R_c = 0.1$.

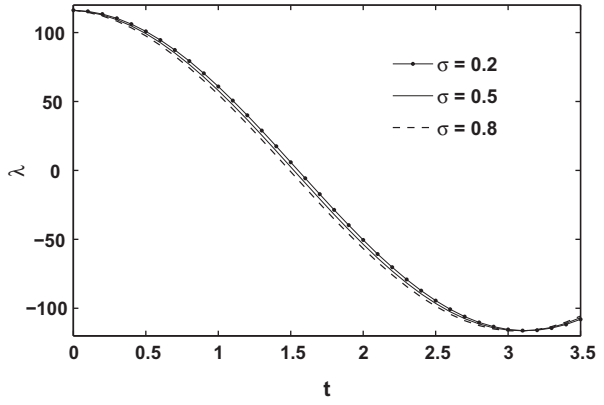

Figure 9 The variation in the resistance to the flow with respect to σ with $\psi = 0.5, \beta = 1.5, Re = 10, \epsilon = 0.1, \omega = 0.2, \zeta = -0.005, \nu = 0.0001, R_c = 0.1$.

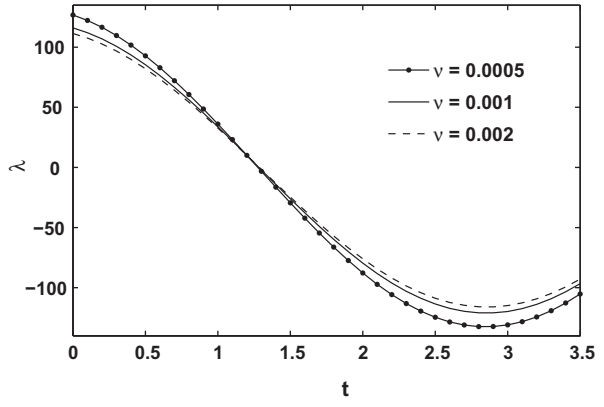

Figure 10 The variation in the resistance to the flow with respect to ν with $\psi = 0.5, \beta = 1.5, \omega = 0.2, \sigma = 3, Re = 10, \epsilon = 0.1, \zeta = -0.005, R_c = 0.1$.

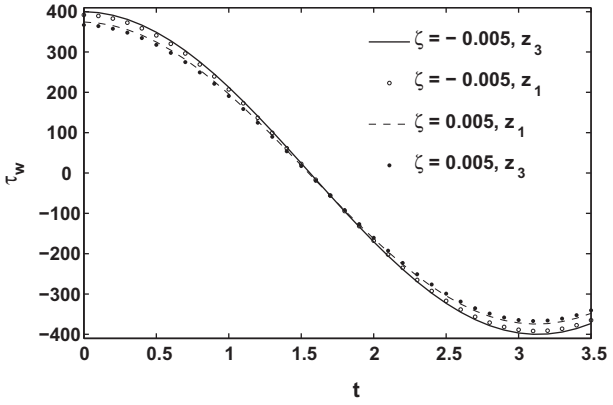

Figure 11 The variation of shear stress at wall with respect to ζ at both maximum height in the stenosis with $\psi = 0.5, \beta = 0.5, \omega = 0.5, \sigma = 0.5, Re = 10, v = 0.0001, \epsilon = 0.1, R_c = 0.1$.

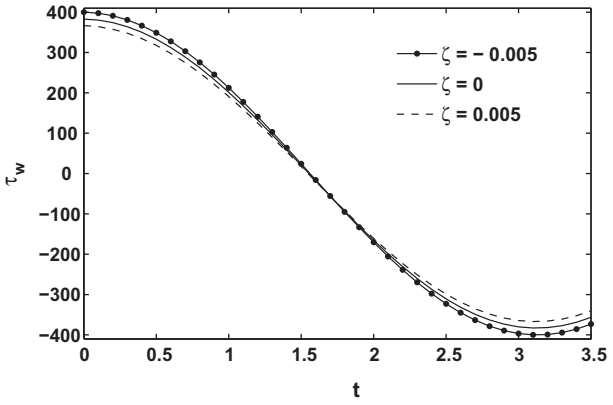

Figure 12 The variation of shear stress at wall with respect to ζ at z_3 with $\psi = 0.5, \beta = 0.5, \omega = 0.5, \sigma = 0.5, Re = 10, \epsilon = 0.1, v = 0.0001, R_c = 0.1$.

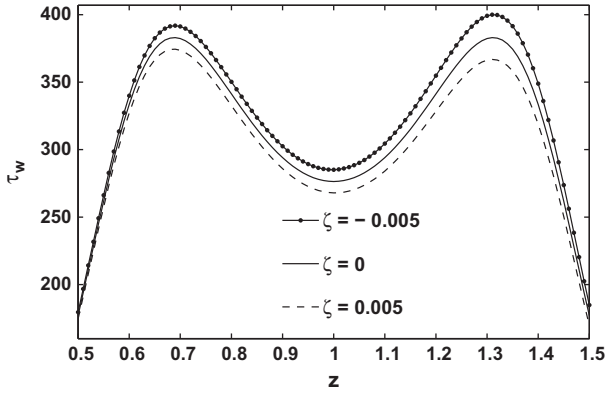

Figure 13 The variation of shear stress at wall in stenosed region with respect to ζ when $\psi = 0.5, \beta = 0.5, \sigma = 0.5, Re = 5, \epsilon = 0.1, \omega = 0.5, v = 0.0001, R_c = 0.1$.

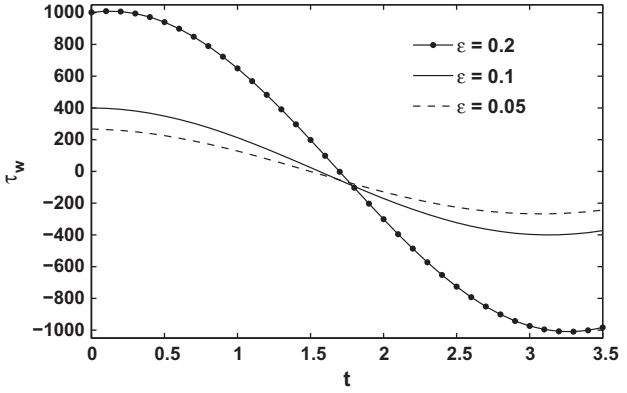

Figure 14 The variation of shear stress at wall with respect to ϵ at z_3 with $\psi = 0.5, \beta = 0.5, \omega = 0.5, \sigma = 0.5, Re = 10, \zeta = -0.005, v = 0.0001, R_c = 0.1$.

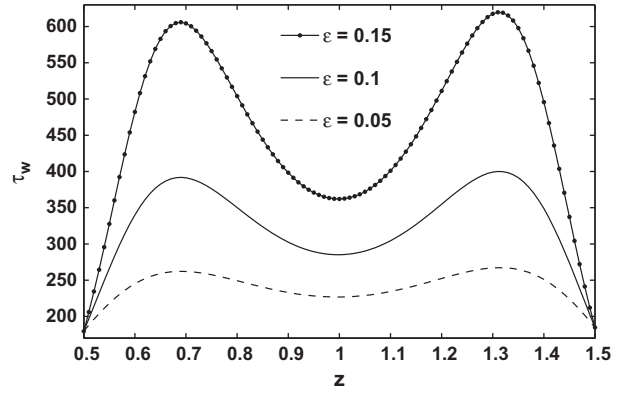

Figure 15 The variation of shear stress at wall in stenosed region with respect to ϵ when $\psi = 0.5, \beta = 0.5, \sigma = 0.5, Re = 5, \omega = 0.5, \zeta = -0.005, v = 0.0001, R_c = 0.1$.

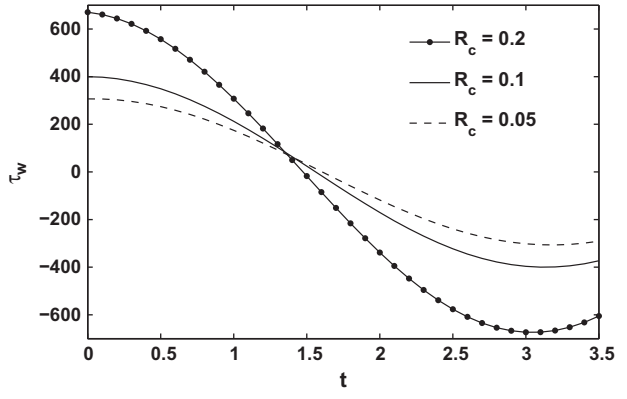

Figure 16 The variation of shear stress at wall with respect to R_c at z_3 with $\psi = 0.5, \beta = 0.5, \omega = 0.5, \sigma = 0.5, Re = 10, \epsilon = 0.1, v = 0.0001, \zeta = -0.005$.

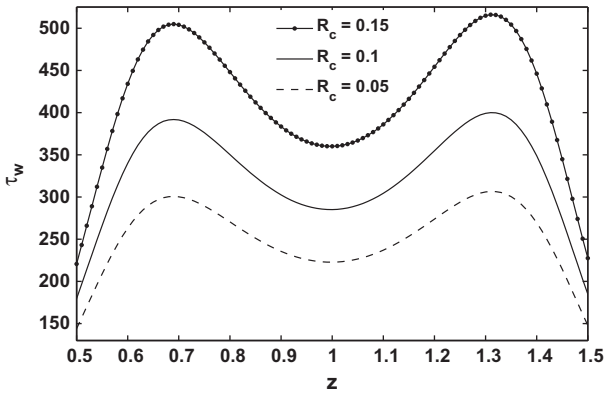

Figure 17 The variation of shear stress at wall in stenosed region with respect to R_c when $\psi = 0.5, \beta = 0.5, \sigma = 0.5, Re = 5, \epsilon = 0.1, \omega = 0.5, v = 0.0001, \zeta = -0.005$.

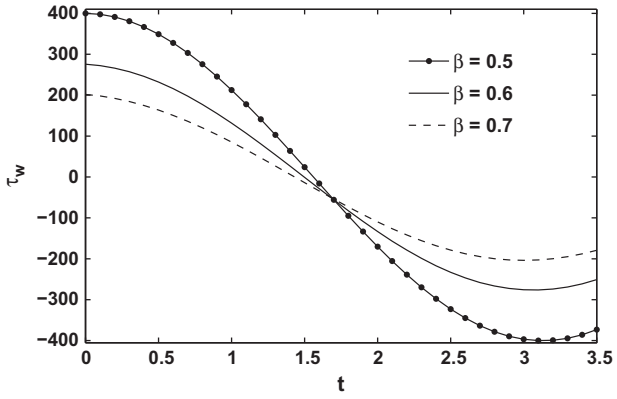

Figure 18 The variation of shear stress at wall with respect to β at z_3 with $\psi = 0.5, \omega = 0.5, \sigma = 0.5, Re = 10, \epsilon = 0.1, \zeta = -0.005, v = 0.0001, R_c = 0.1$.

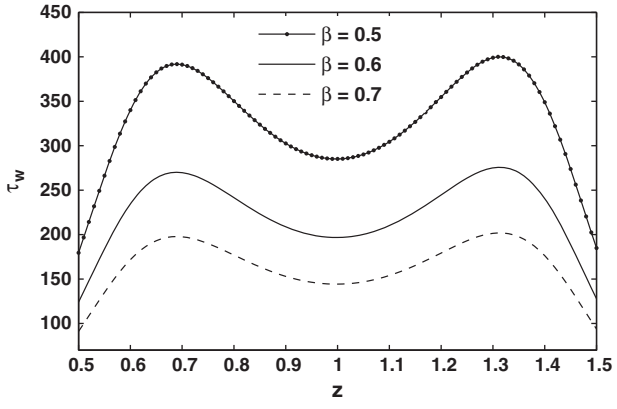

Figure 19 The variation of shear stress at wall in stenosed region with respect to β when $\psi = 0.5, \sigma = 0.5, \epsilon = 0.1, Re = 5, \omega = 0.5, \zeta = -0.005, v = 0.0001, R_c = 0.1$.

The effects of Reynolds number (Re) on impedance are depicted in Fig. 8. From this figure it can be seen that as Reynolds number is increasing impedance is also increasing for small period of time and then starts decreasing. Here it is observed that inertial forces are dominating for small period

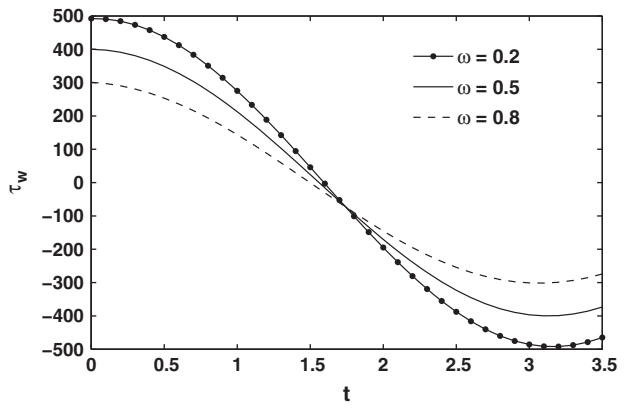

Figure 20 The variation of shear stress at wall with respect to ω at z_3 with $\psi = 0.5, \beta = 0.5, \sigma = 0.5, Re = 10, \epsilon = 0.1, \zeta = -0.005, v = 0.0001, R_c = 0.1$.

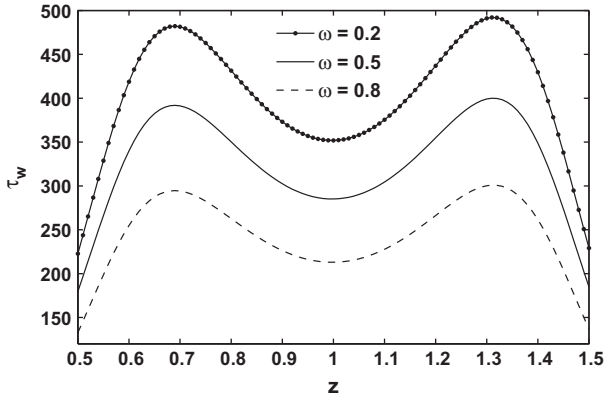

Figure 21 The variation of shear stress at wall in stenosed region with respect to ω when $\psi = 0.5, \beta = 0.5, \sigma = 0.5, Re = 5, \epsilon = 0.1, \zeta = -0.005, v = 0.0001, R_c = 0.1$.

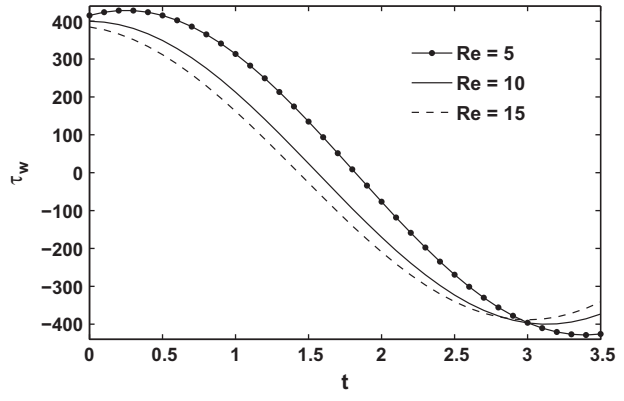

Figure 22 The variation of shear stress at wall with respect to Re at z_3 with $\psi = 0.5, \beta = 0.5, \omega = 0.5, \sigma = 0.5, \epsilon = 0.1, \zeta = -0.005, v = 0.0001, R_c = 0.1$.

of time and later viscous forces seem to be dominating. Same trend is observed in case of Strouhal number (σ) as shown in Fig. 9. It is to be noticed that unsteady forces are

dominating for small period of time while inertial forces are dominating after that small time period. From these two results it appears that the separation of flow moves towards the value of z where the maximum height of the stenosis occurs. Womersely number effect can be understood as it is the product of Reynolds number (Re) and Strouhal number (σ). Significant effect of slip velocity at the arterial wall on the impedance is studied from Fig. 10. Here it is observed that in case of high slip velocity impedance is less. Hence no-slip at the wall of the artery makes the fluid to stick to the boundary thus providing more resistance to the blood flow.

For the analysis of the blood flow characteristics through stenotic tapered artery, wall shear stress is an important diagnostic element. It has significant role in the development of arterial diseases. In case of high wall shear stress, inner wall of the artery (intima) can damage. The development of wall shear stresses is related to the progress and decay of the endothelial cells of the arterial wall [39–41]. Hence, appearance of wall shear stress is imperative in the analysis of the arterial diseases. The location of critical and extreme heights of stenosis which are dependent on the tapered parameter have been computed and summarized in the form of Table 1. It is also observed that the locations of the extreme heights have different impact on the shear stress at the wall. The same has been depicted in Fig. 11. Here it is observed that for a converging tapered artery the shear stress is maximum at z_3 and the trend is reversed in case of diverging tapered artery. Since high wall shear stress impacts the inner wall of the artery it is important to consider the effect of wall shear stress at the maximum height of stenosis where high shear stress occurs and this is very likely to happen at either z_1 or z_3. Hence further discussions are done at these locations.

From the Figs. 12 and 13, it is clear that the converging tapered artery is accounting for more shear stress at the wall when compared to diverging and non-tapered artery. Further it is also observed that shear stress at the wall is same at both the locations of maximum height in case of non-tapered artery as depicted in Fig. 13. From the same figure it is also observed that there is variation in shear stress in case of tapered arteries. Having understood the effect of the location and the tapering angle, all further analysis has been done at z_3 corresponding to converging tapered artery. Hence all further results for wall shear stress are computed for the fixed value of the tapered parameter ($\zeta = -0.005$).

Figs. 14 and 15 describe the effect of ϵ on the wall shear stress at the maximum height of the stenosis and across the entire stenotic region respectively. It is noticed that as height of the stenosis increases shear stress also increases. Further it is maximum at the locations corresponding to the extreme heights. Insertion of catheter in the stenosed artery has significant effect on the flow dynamics in lumen of the artery. Increment in the radius of catheter reduces the annular region of the artery. Therefore, pressure on the wall effectively increases and may damage the inner wall of the artery. Hence the influence of catheter radius deserves to be noticed and is exhibited through Figs. 16 and 17. It is worth noting that the shear stress at the wall is maximum when a thick catheter is introduced in a converging tapered artery. As the couple stress fluid parameter (β) approaches to infinity the fluid starts assuming the Newtonian behaviour. Hence it is expected that wall shear stress is very small in case of Newtonian fluid when compared to couple stress fluid. Further as $\omega(=\eta'/\eta)$ is approaching towards unity the wall shear stress is decreasing. Further as $\omega \to 1$, the stress tensor

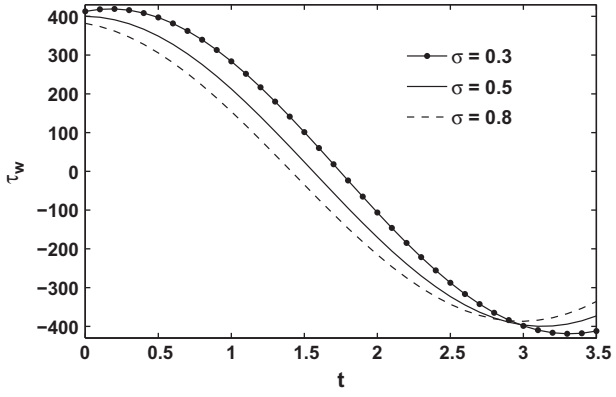

Figure 24 The variation of shear stress at wall with respect to σ at z_3 with $R_c = 0.1, \beta = 0.5, \omega = 0.2, Re = 10, \epsilon = 0.1, \zeta = -0.005, v = 0.0001, R_c = 0.1$.

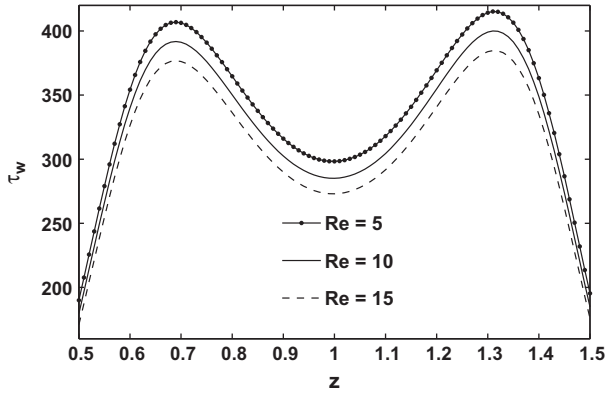

Figure 23 The variation of shear stress at wall in stenosed region with respect to Re when $\psi = 0.5, \beta = 0.5, \sigma = 0.5, \epsilon = 0.1, \omega = 0.5, \zeta = -0.005, v = 0.0001, R_c = 0.1$.

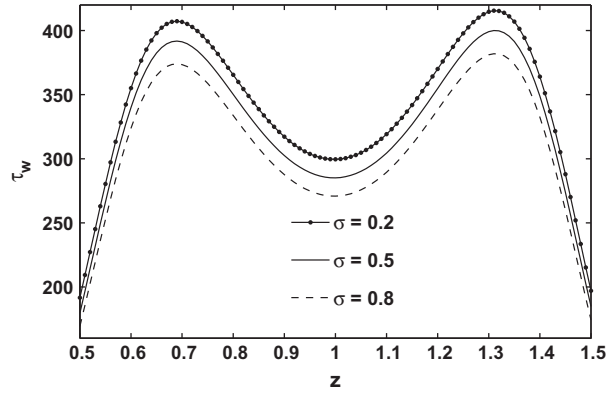

Figure 25 The variation of shear stress at wall in stenosed region with respect to σ when $\psi = 0.5, \beta = 0.5, \epsilon = 0.1, Re = 5, \omega = 0.5, \zeta = -0.005, v = 0.0001, R_c = 0.1$.

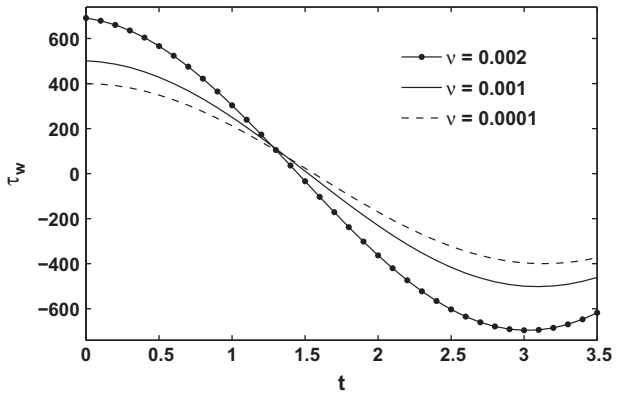

Figure 26 The variation of shear stress at wall with respect to ν at z_3 with $\psi = 0.5, \omega = 0.5, \sigma = 0.5, Re = 10, \epsilon = 0.1, \zeta = -0.005, R_c = 0.1$.

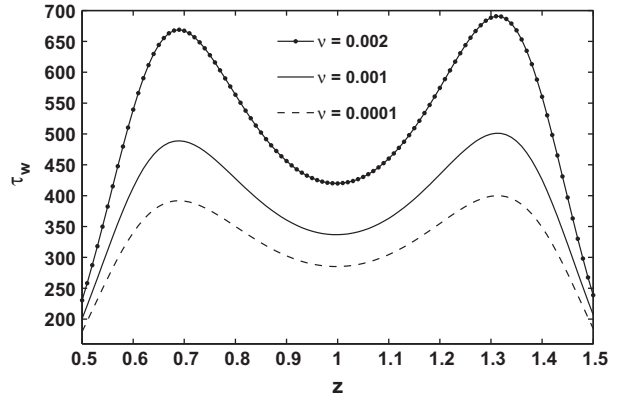

Figure 27 The variation of shear stress at wall in stenosed region with respect to ν when $\psi = 0.5, \sigma = 0.5, \epsilon = 0.1, Re = 5, \omega = 0.5, \zeta = -0.005, R_c = 0.1$.

becomes symmetric. Hence couple stress fluid for which shear stress tensor is asymmetric has more wall shear stress. The above behaviours are sketched in Figs. 18–21. The effects of Reynolds number (Re) and Strouhal number (σ) on wall shear stress are depicted in Figs. 22–25. It is observed that their effects on wall shear stress are similar to that of their effects on impedance. Finally the effect of velocity slip on the shear stress at the wall is understood from Figs. 26 and 27. As the velocity slip at the wall increases, the stickiness of the fluid at the wall gets reduced, resulting in high flow velocity. This results in high wall shear stress.

5. Conclusion

There is a special importance to non-Newtonian fluid than the Newtonian fluid because of its wide existence such as oil, blood and polymeric solutions. In view of the above an analytical approach was followed to solve the mathematical model of blood flow through stenosed tapered artery under the assumption of mild stenosis. In a nutshell, the main observations are

- The locations of the extremum heights are different for different tapering angles. It is important to observe that impedance and shear stress at wall are significantly depending on these noticed locations.
- Rise in slip velocity reduces the impedance significantly and at the same time increases the shear stress at the wall.
- The couple stress fluid model is the most generalized model because couple stress fluid will behave like classical Newtonian fluid with certain extreme conditions.
- The present study enables us to understand mathematically the variation in impedance and wall shear stress with respect to fluid and geometric parameters.

The modelling and simulation of the above phenomena is very realistic and is expected to be very useful in predicting the behaviour of physiological parameters in the diagnosis of various arterial diseases.

Acknowledgments

Authors are grateful to the editor and reviewers for their suggestions and comments for the improvement of the manuscript.

References

[1] Lim SS, Vos T, et al. A comparative risk assessment of burden of disease and injury attributable to 67 risk factors and risk factor clusters in 21 regions, 1990–2010: a systematic analysis for the Global Burden of Disease Study 2010. The Lancet 2012;380:2224–60.
[2] Young DF. Fluid mechanics of arterial stenosis. J Biomech Eng 1979;101:157–75.
[3] Young DF. Effect of a time-dependent stenosis on flow through a tube. J Manuf Sci Eng 1968;90:248–54.
[4] Young DF, Tsai FY. Flow characteristics in models of arterial stenosis I. Steady flow. J Biomech 1973;6:395–402.
[5] Padmanabhan N. Mathematical model of arterial stenosis. Med Biol Eng Comput 1980;18:281–6.
[6] Cokelet GR. The rheology of human blood. Massachusetts Ins of Tech; 1963.
[7] Haynes RH. Physical basis of the dependence of blood viscosity on tube radius. Am J Physiol 1960;198:1193–200.
[8] Siddiqui SU, Verma NK, Shailesh Mishra, Gupta RS. Mathematical modelling of pulsatile flow of Casson's fluid in arterial stenosis. App Math Comp 2009;210:1–10.
[9] Sankar DS, Usik Lee. Mathematical modeling of pulsatile flow of non-Newtonian fluid in stenosed arteries. Commun Nonlinear Sci Numer Simul 2009;14:2971–81.
[10] Varshney G, Katiyar VK, Sushil Kumar. Numerical modelling of pulsatile flow of blood through a stenosed tapered artery under periodic body acceleration. J Mech Med Biol 2010;10:251–72.
[11] Akbar NS, Hayat T, Nadeem S, Hendi AA. Influence of mixed convection on blood flow of Jeffrey fluid through a tapered stenosed artery. J Thermal Sci 2013;17:533–46.
[12] Akbar NS, Nadeem S. Influence of heat and chemical reactions on the Sisko fluid model for blood flow through a tapered artery with a mild stenosis. Quaest Math 2014;37:157–77.
[13] Akbar NS. Blood flow analysis of Prandtl fluid model in tapered stenosed arteries. Ain Shams Eng J 2014;5:1267–75.
[14] Chakravarty S, Mandal PK. Two-dimensional blood flow through tapered arteries under stenotic conditions. Int J Non-Linear Mech 2000;35:779–93.

[15] Akbar NS, Rahman SU, Ellahi R, Nadeem S. Nano fluid flow in tapering stenosed arteries with permeable walls. Int J Thermal Sci 2014;85:54–61.
[16] Akbar NS, Nadeem S, Hayat T, Alsaedi A. Heat transfer analysis for the peristaltic flow of chyme in small intestine: a theoretical study. J Mech Med Biol 2012;12. http://dx.doi.org/10.1142/S021951941100471X.
[17] Sankar DS, Hemalatha K. Pulsatile flow of Herschel–Bulkley fluid through catheterized arteries – a mathematical model. App Math Modell 2007;31:1497–517.
[18] Srinivasacharya D, Srikanth D. Effect of couple stresses on the pulsatile flow through a constricted annulus. Comp Rendus Mec 2008;336:820–7.
[19] Riahi DN, Ranadhir R, Sam Cavazos. On arterial blood flow in the presence of an overlapping stenosis. Math Comput Model 2011;54:2999–3006.
[20] Srivastava VP, Mishra S. Non-Newtonian arterial blood flow through an overlapping stenosis. App App Math: An Int J 2010;5:225–38.
[21] Chakravarty S, Mandal PK. Mathematical modeling of blood flow through an overlapping stenosis. Math Comput Model 1994;19:59–70.
[22] Vand V. Viscosity of solutions and suspensions. I. Theory. J Phys Chem 1948;52:277–99.
[23] Bunnett L. Red cell slip at a wall in vitro. Science 1967;24:1554–6.
[24] Nubar Y. Blood flow, slip, and viscometry. Biophys J 1971;11:252–64.
[25] Chaturani P, Biswas D. A comparative study of Poiseuille flow of a polar fluid under various boundary conditions with applications to blood flow. Rheol Acta 1984;23:435–45.
[26] Ponalagusamy R. Blood flow through an artery with mild stenosis: a Two-layered model, different shapes of Stenoses and slip velocity at the wall. J Appl Sci 2007;7:1071–7.
[27] Biswas D, Chakraborty US. Pulsatile flow of blood in a constricted artery with body acceleration. App App Math: An Int J 2009;4:329–42.
[28] Ponalagusamy R, Tamil Selvi R. Blood flow in stenosed arteries with radially variable viscosity, peripheral plasma layer thickness and magnetic field. Meccanica 2013;48:2427–38.
[29] Sukhendu Ghosh, Usha R, Kirti Chandra Sahu. Linear stability analysis of miscible two-fluid ow in a channel with velocity slip at the walls. Phys Fluids 2014;26:014107.
[30] Stokes VK. Theories of fluids with microstructure: an introduction. Berlin, Heidelberg: Springer-Verlag; 1984.
[31] Eringen AC. Theory of micropolar fluids. No. RR-27. Purdue Univ Lafayette in School of Aeronautics and Astronautics; 1965.
[32] Cowin SC. The theory of polar fluids. Adv Appl Mech 1975;14:279–82.
[33] Pralhad RN, Schultz D. Modeling of arterial stenosis and its applications to blood diseases. Math Biosci 2004;190:203–20.
[34] Srinivasacharya D, Srikanth D. Effect of couple stresses on the flow in a constricted annulus. Arch Appl Mech 2008;78:251–7.
[35] Srikanth D, Kebede Tedesse. Mathematical analysis of non-Newtonian fluid flow through multiple stenotic artery in the presence of catheter-a pulsatile flow. Int J Non-linear Sci 2012;13:15–27.
[36] Srivastava LM. Flow of couple stress fluid through stenotic blood vessels. J Biomech 1985;18:479–85.
[37] Logerfo FW, Crawshaw HM, Nowak M, Serrallach E, Quist WC, Valeri CR. Effect of flow split on separation and stagnation in a model vascular bifurcation. Stroke 1981;12:660–5.
[38] Smith FT. The separating flow through a severely constricted symmetric tube. J Fluid Mech 1979;90:725–54.
[39] Ku DN. Blood flow in arteries. Annu Rev Fluid Mech 1997;29:399–434.
[40] Glagov S, Zarins C, Giddens DP, Ku DN. Hemodynamics and atherosclerosis. Insights perspectives gained from studies of human arteries. Arch Pathol Lab Med 1988;112:1018–31.
[41] Fry DL. Acute vascular endothelial changes associated with increased blood velocity gradients. Circul Res 1968;22:165–97.

Dr. D Srikanth, PhD, Assistant Professor, Department of Applied Mathematics, Defence Institute of Advanced Technology, Pune, India.

Mr. J.V. Ramana Reddy, Research Sholar, Department of Applied Mathematics, Defence Institute of Advanced Technology, Pune, India.

Ms. Shubha Jain, M.Tech. Project Student, Department of Applied Mathematics, Defence Institute of Advanced Technology, Pune, India.

Dr. Anup Kale, PhD, Assistant Professor, Department of Bio-Sciences, Defence Institute of Advanced Technology, Pune, India.